MATEC Web of Conferences **33**, 05001 (2015)
DOI: 10.1051/matecconf/20153305001

Magnetic states of C-doped $Ni_{43.75}Co_{6.25}Mn_{37.5}In_{12.5}$ Heusler alloys

Vasiliy Buchelnikov[1,a], Vladimir Sokolovskiy[1] and Peter Entel[2]

[1]*Chelyabinsk State University, Condensed Matter Department, 454001 Chelyabinsk, Russia*
[2]*University of Duisburg-Essen, Faculty of Physics and Center for Nanointegration, CENIDE, D-47048 Duisburg, Germany*

Abstract. In this study, we present the results of first principles calculations of structural and magnetic equilibrium states of carbon doped $Ni_{1.75}Co_{0.25}Mn_{1.5}In_{0.5}$ Heusler alloy. The pseudopotential method within spin-polarized generalized gradient approximation is used. Different distributions of Mn, In and C atoms as well as different spin reference states are discussed by using a supercell approach. The ferromagnetic cubic austenite with substitution of C for Mn is found to be energetically stable. The addition of carbon has promoted the martensitic transformation from a ferromagnetic cubic structure to a ferrimagnetic tetragonal structure with *c/a* ratio of 1.35.

1 Introduction

Nowadays, ferromagnetic (FM) shape memory Ni-Mn-Z (Z = Ga, In, Sn, Sb) Heusler alloys are promising candidates for a new class of functional materials. The ever-growing attention of theorists and experimentalists is associated with the observation in these alloys of many interesting phenomena such as giant magnetocaloric effect (MCE), large magnetoresistance, magnetic field-induced strain, and exchange bias [1-10]. It is common knowledge that the magnetic and structural properties of Heusler alloys are very sensitive to the content of Mn because the Mn excess atoms substitute for Z on the Z sublattice of the X_2YZ Heusler structure. It is generally believed that in the nonstoichiometric case, $Ni_2Mn_{1+x}Z_{1-x}$, the Mn excess atoms can interact antiferromagnetically (AFM) with the surrounding Mn atoms on the regular Mn sublattice due to the much shorter Mn_Y-Mn_Z distance as against the $Mn_{Y(Z)}$ -$Mn_{Y(Z)}$ distances. Here Mn_Y and Mn_Z refer to Mn located on the original Mn sites and on the Z sites, respectively.

In the past five years considerable information has been accumulated on the influence of substituting an additional element such as Co, Fe, Si, B, etc. on the physical properties of Ni-Mn-Z Heusler alloys [10-17]. It is known that the additional element can change smoothly or sharply both the magnetic and structural phase transitions to bring about a transformation sequence from martensite with low magnetization to FM austenite and to lead to better magnetocaloric properties [10-17]. The breakthrough in the field of MCE has been recently achieved by Liu et al. [13] who have observed the giant inverse MCE ($\Delta T_{ad} \approx$ -6.2 K) with $Ni_{45}Co_5Mn_{37}In_{13}$ in a magnetic field change of 1.9 T. So far, this is the record value among all Heusler alloys. On the other hand, it was obtained only in the first cycle of applying a field and ΔT_{ad} is reduced on subsequent cycles due to thermal hysteresis. As shown by Liu et al. [13], one way to overcome the hysteresis problem may be the application of external pressure. It turns out that if the sample is magnetized without bias stress but demagnetized under a low external hydrostatic pressure of 1.3 kbar, the magnetic hysteresis can be significantly reduced. Therefore, the relative cooling power can be increased by simultaneously varying magnetic field and pressure compared with the cooling power achieved when only the magnetic field is varied.

Another method to resolve the problem of thermal hysteresis as well as to optimize the MCE is appropriate doping. For instance, carbon can be used as a potential dopant for Ni-Co-Mn-In alloys. Our interest to carbon addition is related with the fact that it may result in a carbide formation like NiC or MnC which may act as lubricant hindering kinetic arrest phenomena, such lubricant features are well known for Ti-Fe-C etc. [18]. Before the theoretical modelling of thermal hysteresis as well as MCE by the Monte Carlo method we need to determine the magnetic and structural equilibrium states of Ni-Co-Mn-In-C alloy. In this work, we investigate the effect of carbon substitution at different sites on equilibrium states of $Ni_7Co_1Mn_6In_2$ ($Ni_{43.75}Co_{6.25}Mn_{37.5}In_{12.5}$) by using a supercell approach.

2 Computational methods

The electronic structure has been calculated by using the Quantum Espresso (QE) package [19]. The interactions between the atomic core and the valence electrons were described by the ultrasoft pseudopotentials (RRKJUS) with high number of valence electrons [19]. The generalized gradient approximation (GGA) in the formulation of Perdew, Burke and Ernzerhof (PBE) for

[a] Corresponding author: buche@csu.ru

the representation of the exchange-correlation functional was used [20]. The structural optimizations are performed using the Broyden-Fletcher-Goldfarb-Shanno algorithm [19]. The Kohn-Sham orbitals were described using a plane-wave basis set. An energy cut-off of 80 Ry was used to truncate the plane-wave expansion of the electronic wave functions. The charge-density cut-off was kept at 12.5 times that of the kinetic energy cut-off and the Methfessel-Paxton smearing size was fixed at 5 mRy. In the calculations we used automatically generated uniform ***k***-point grid similar to Monkhorst-Pack grids. The modeling parameters are calculated after an energy convergence of 0.01 mRy. The Brillouin zone integration was carried out using smearing with Methfessel-Paxton first-order spreading. A denser k-point mesh of 8^3 and "smearing" and "tetrahedra" occupations mode were used for the lattice relaxation and tetragonal distortion calculations, respectively.

In order to determine the magnetic ground state and equilibrium lattice parameter of carbon doped Ni-Co-Mn-In alloy in the austenite, the energy calculations were carried out using a 16-atom supercell of the $Ni_7Co_1Mn_6In_1C_1$ alloy. Here, three situations of atomic distribution of $Mn_{Y(Z)}$, In and C atoms were considered, (Fig. 1). In the first and second cases (Figs. 1(a, b)), one Mn_Y atom at the centre of the cubic cell replaces by C and goes to either of two In sites. As the result, in the first case C has two nearest neighbours (*nn*) Mn_Z and three next nearest neighbours (*nnn*) Mn_Y atoms. For second case, C has two *nn* Mn_Y and three *nnn* Mn_Z atoms, respectively. Finally, in the third case (Fig. 1(c)), one In atom replaces by C atom. We denoted described atomic distributions as follows: C(2*nn*Mn_Z), C(3*nn*Mn_Z) and C(In), respectively. It should be noted that other atomic distributions would be equivalent to these ones.

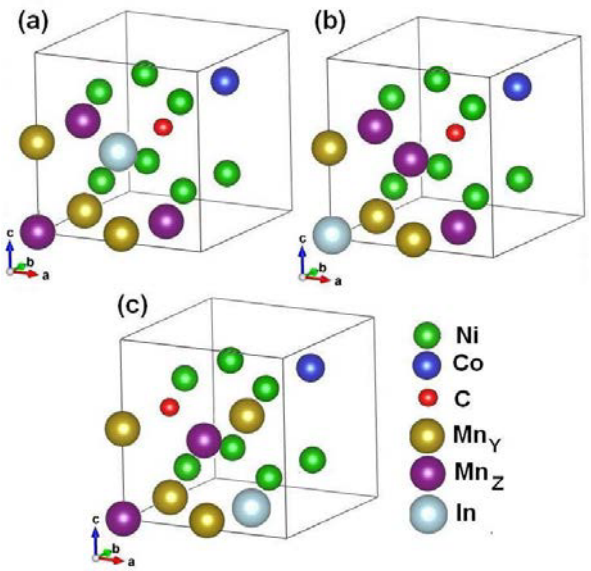

Figure 1. (Color online) Three types of 16-atom supercells for off-stoichiometric $Ni_7Co_1Mn_6In_1C_1$ Heusler alloy were used. Here (a) C(2*nn*Mn_Z) (b) C(3*nn*Mn_Z) and (c) C(In) are different atomic distributions.

Two magnetic configurations for the energy calculations were also considered. The first one was the FM state, in which all magnetic moments of Ni, Co Mn_Y and Mn_Z atoms are positive. The second one was a ferrimagnetic (FIM) phase with the positive magnetic moments of Ni, Co and Mn_Y atoms and the negative magnetic moment of Mn_Z atoms.

3 Results and discussions

In the first step, the lattice constants were determined for different spin configurations. The total energies as functions of the lattice parameter and tetragonal *c*/*a* ratio for both FM and FIM states are calculated and presented in Figs. 2 and 3.

Let us first discuss the lattice relaxation calculations. As can clearly be seen from Fig. 2, the FM austenite with C(2*nn*Mn_Z) atomic configuration is found to be more stable in energy compared with other cases although the small difference in energy (≈ 10 meV/f.u.) between the FM austenite with C(In) and C(2*nn*Mn_Z) atomic distributions. It has be pointed out that the carbon addition in $Ni_7Co_1Mn_6In_2$ alloy results in a decrease in equilibrium lattice parameter from $a_0 \approx 5.96$ Å (C 0 at.%) up to 5.85 Å (C 6.25 at.%). The value of 5.96 Å has been estimated theoretically from *ab initio* relaxation calculations presented in Refs. [21, 22].

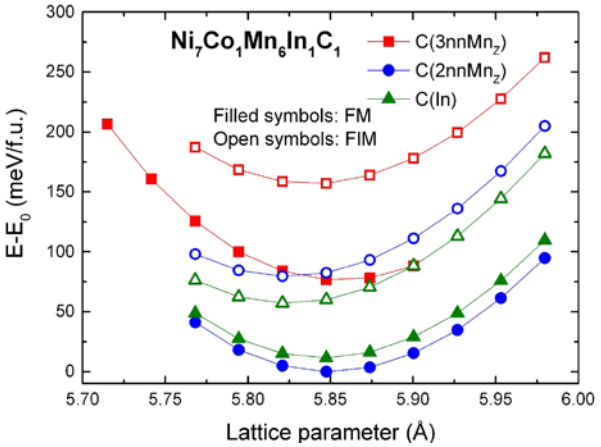

Figure 2. (Color online) The variation of the total energy per formula unit (f.u. - 4 atoms) of $Ni_7Co_1Mn_6In_1C_1$ alloy for different supercells with FM and FIM spin configurations. Here, E_0 is the equilibrium total energy for the FM C(2*nn*Mn_Z) atomic configuration. Results for FM and FIM orders are depicted by lines with filled and open symbols, respectively.

The equilibrium lattice constants and bulk moduli of cubic C-doped $Ni_7Co_1Mn_6In_2$ alloy calculated for different supercells and spin configurations are listed in Table 1. Here, the lattice parameter was derived by minimizing the total energy while the bulk modulus has been calculated from the double derivative of the total energy (*E*), by using the following equation.

$$B = -V_0\left(\frac{\partial P}{\partial V}\right) = V_0\left(\frac{\partial^2 E}{\partial V^2}\right) \quad (1)$$

Here V_0 is the equlibrium volume, P and V are the external pressure and the cell volume, respectively.

Table 1. Equilibrium lattice parameters and bulk moduli of the cubic C-doped $Ni_7Co_1Mn_6In_2$ alloy with different spin reference states.

Compound	spin order	a_0 (Å)	B (GPa)	M (μ_B/f.u.)
$Ni_7Co_1Mn_6In_2$	FM	5.969	136.95	6.825
$Ni_7Co_1Mn_6In_2$	FIM	5.961	134.02	2.365
C(In)	FM	5.845	144.92	6.893
C(In)	FIM	5.825	139.53	2.342
C(2*nn*Mn_Z)	FM	5.848	145.62	6.933
C(2*nn*Mn_Z)	FIM	5.824	140.23	0.4
C(3*nn*Mn_Z)	FM	5.855	148.17	7.02
C(3*nn*Mn_Z)	FIM	5.838	141.3	0.097

Concerning the bulk modulus, it can be seen from Table 1 that it increases with decreasing of the lattice parameter due to the carbon addition in $Ni_7Co_1Mn_6In_2$ alloy. The largest bulk modulus ($B \approx 148.17$ GPa) is found for the FM austenite with C(3*nn*Mn_Z) atomic distribution. With respect to the total magnetic moment, it is seen from Table 1 that the carbon doping leads to an increase (decrease) in the magnetic moment of FM (FIM) austenite, respectively. Small values of magnetic moment obtained for FIM austenite with C(2*nn*Mn_Z) and C(3*nn*Mn_Z) atomic distributions are due to the increase of Mn_Z atoms interacting with Mn_Y atoms antiferromagnetically. It should be noted that the equilibrium lattice parameter and magnetization determined with *ab initio* calculations reported in Table 1 are in good agreement with experimental data [13].

Using the equilibrium lattice parameter and keeping a constant volume, the variation of the total energy as a function of tetragonal distortion of $Ni_7Co_1Mn_6In_1C_1$ alloy with C(In) and C(2*nn*Mn_Z) atomic configurations are presented in Fig. 3(a, b). In order to see the effect of C on martesitic phase transition in a C-doped NiCoMnIn alloy, the energy curve calculated for the $Ni_7Co_1Mn_6In_2$ composition is also presented in Fig. 3(c).

From Fig. 3(a), it can be seen that there are two energy minima at c/a = 0.95 and 1.33 for the FIM spin configuration in $Ni_7Co_1Mn_6In_1C_1$ alloy with C(2*nn*Mn_Z) atomic distribution. With respect the FM alignment, we can observe only one energy minimum at c/a ratio of 0.97. On the other hand, in the case of $Ni_7Co_1Mn_6In_1C_1$ alloy with C(In) atomic distribution (Fig. 3(b)), it is seen that there is one energy minimum at c/a of 1.19 (FM state) and 1.35 (FIM state). Finally, in the case of $Ni_7Co_1Mn_6In_2$ alloy, the FM austenite is energetically favorable as compared with the FIM martensite, which has the energy minimum at c/a ratio of 1.25. Evidently, the carbon addition stimulates the martensitic phase transformation in composition $Ni_7Co_1Mn_6In_2$ at a Co content of 6.25 at.%. We would like to note that in case of NiCoMnIn compositions, the martensitic transformation occurs experimentally at smaller content of Co [10]. In general, the substitution of (6.25 at.%) C and Co for Mn and Ni results in the martensitic transformation from FM cubic austenite to FIM tetragonal martensite due to the fact that the energy difference between the austenitic and martensitic structures is large for both compositions (See, Fig. 3(a, b)).

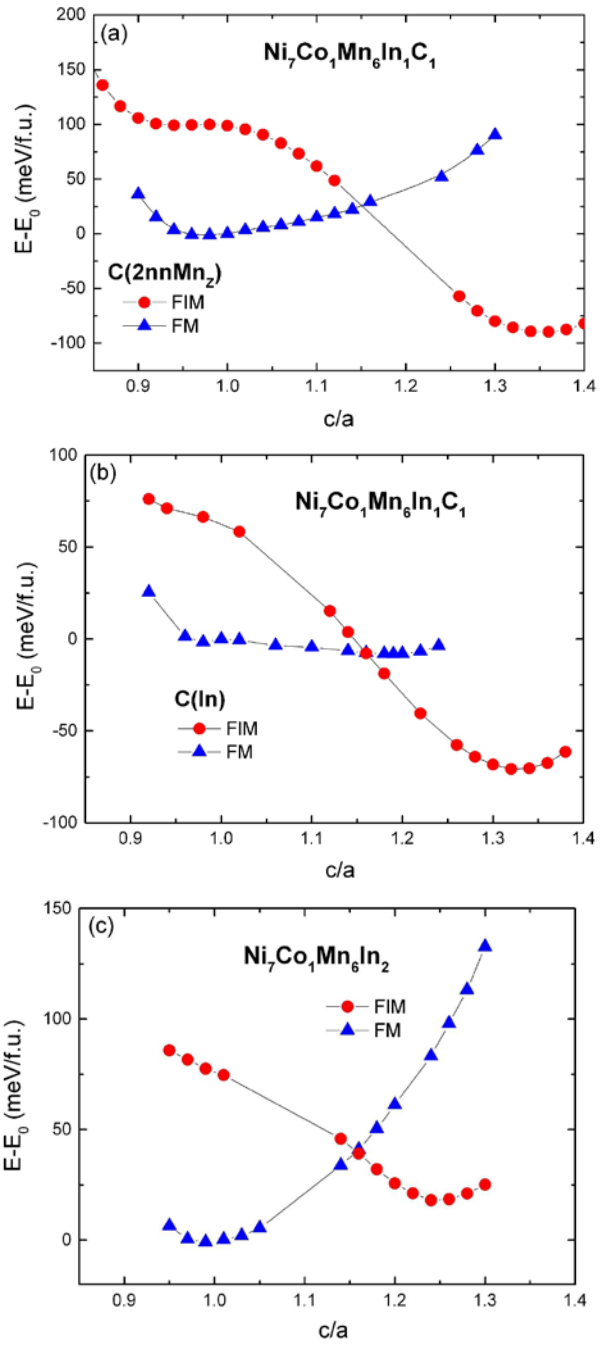

Figure 3. (Color online) Relative variation of the total energy as a function of the tetragonality in $Ni_7Co_1Mn_6In_1C_1$ alloy with (a) C(2*nn*Mn_Z) and (b) C(In) atomic configurations and (c) $Ni_7Co_1Mn_6In_2$ alloy. Zero energy corresponds to the energy of the $L2_1$ structure in each case.

The total magnetic moments in martensitic phases with FM and FIM spin alignments in dependence on the carbon substitution in NiCoMnIn alloys are listed in Table 2.

Table 2. Total magnetic moments in the martensitic states of C-doped $Ni_7Co_1Mn_6In_2$ alloy with different spin reference states.

Compound	spin order	*c*/*a*	*M* (μ_B/f.u.)
$Ni_7Co_1Mn_6In_2$	FIM	1.25	2.13
C(In)	FM	1.19	6.63
C(In)	FIM	1.33	2.07
C(2*nn*Mn_Z)	FM	0.97	6.88
C(2*nn*Mn_Z)	FIM	1.35	0.39

As can be seen from Table 2, the smallest magnetization is found in the FIM martensite with C(2*nn*Mn_Z) atomic distribution. The small value of magnetization is related with a shorter distance between Mn_Y and Mn_Z atoms interacting antiferromagnetically. Besides, the number of Mn_Z atoms in the composition with C(2*nn*Mn_Z) atomic distribution is greater by one than in the composition with C doped for In. Comparing with the results obtained for $Ni_7Co_1Mn_6In_2$ alloy, it is seen that the largest difference in magnetization between austenite and martensite is realized with the carbon doping for Mn. Therefore, better magnetocaloric properties can be expected.

4 Summary

In this work the equilibrium magnetic and structural ground states of C-doped $Ni_7Co_1Mn_6In_2$ composition have been studied by means of the *ab initio* calculations in combination with the supercell approach. Three supercells with different spin configurations and different substitution of C for In and Mn atoms have been considered. It has been shown that the addition of carbon leads to an appearance of martensitic transformation from FM austenite to FIM martensite. Comparing the results obtained from the lattice relaxation calculations, it was showed that the FM austenite with C(2*nn*Mn_Z) atomic configuration has the minimum energy although the FM austenite with C doped for In is very close in energy with the first one. The decrease (increase) in the equilibrium lattice parameter (bulk modulus) was found with carbon addition due to smaller atomic radius of carbon, respectively. Concerning the magnetic moment, it has been shown that the magnetization change between FM austenite and FIM martensite with C(2*nn*Mn_Z) atomic configuration is 6.49 μ_B/f.u. As a result, large magnetocaloric properties can be expected in the C-doped NiCoMnIn system. Additional calculations with the help of Monte Carlo technique of magnetic and magnetocaloric properties as well as thermal hysteresis in C-doped NiCoMnIn system would be needed.

Acknowledgments

This work is supported by RFBR Grant No. 14-02-01085, RSF No. 14-12-00570\14 (Section 2), Ministry of Education and Science of Russian Federation (RF) No 3.2021.2014/K (Section 3). PE acknowledges DFG (SPP 1599) for financial support.

References

1. A.N. Vasiliev, V.D. Buchelnikov, T. Takagi, V.V. Khovailo and E.I. Estrin, Physics-Uspekhi **46**, 559 (2003)
2. T. Krenke, M. Acet, E.F. Wassermann, X. Moya, Ll. Manosa, A. Planes, Nature Mater. **4**, 450 (2005).
3. R. Kainuma, Y. Imano, W. Ito, Y. Sutou, H. Morito, S. Okamoto, O. Kitakami, K. Oikawa, A. Fujita, T. Kanomata, K. Ishida, Nature **493**, 957 (2006)
4. A. Planes, Ll. Manosa, Mater. Sci. Forum **512**, 145 (2006).
5. V.D. Buchelnikov, A.N. Vasiliev, V.V. Koledov, S.V. Taskaev, V.V. Khovaylo, V.G. Shavrov, Physics – Uspechi **49**, 871 (2006)
6. M. Khan, I. Dubenko, S. Stadler, N. Ali, J. Phys. Condens. Matter **20**, 235204 (2008)
7. A. Planes, Ll. Manosa, M. Acet, J. Phys. Condens. Matter **21**, 233201 (2009)
8. V.D. Buchelnikov, and V.V. Sokolovskiy, Phys. Metal. Metallogrh. **112**, 633 (2011).
9. P. Entel, M.E. Gruner, A. Hutch, A. Dannenberg, M. Siewert, H.C. Herper, T. Kakeshita, T. Fukuda, V.V. Sokolovskiy, V.D. Buchelnikov, *in Disorder and Strain-Induced Complexity, Functional Materials* vol. 148 ed. by T. Kakeshita, T. Fukuda, A. Saxena, A. Planes (Springer, Berlin, 2012).
10. V.V. Sokolovskiy, M.A. Zagrebin, V.D. Buchelnikov, in Shape Memory Alloys: Properties, Technologies, Opportunities vol. 81-82, ed. by N. Resnina, V. Rubanik (Mater. Sci. Foundation, TTP, Pfaffikon, 2015).
11. R. Das, S. Sarma, A. Perumal, A. Srinivasan, J. Appl. Phys. **109**, 07A901 (2011)
12. D.Y. Cong, S. Roth, L. Shultz, Acta Mater. **60**, 5335 (2012)
13. J. Liu, T. Gottshall, K. Skokov, J.D. Moore, O. Gutfleisch, Nature Mat. **11**, 620 (2012)
14. I. Dubenko, T. Samanta, A. Quetz, A. Kazakov, I. Rodionov, D. Mettus, V. Prudnikov, S. Stadler, P. Adams, J. Prestigiacomo, A. Granovsky, A. Zhukov, N. Ali, Appl. Phys. Lett. **100**, 192402 (2012).
15. I. Dubenko, T. Samanta, A.K. Pathak, A. Kazakov, V. Prudnikov, S. Stadler, A. Granovsky, A. Zhukov, N. Ali, J. Magn. Magn. Mater. **324**, 3530 (2012).
16. R.Y. Umetsu, D. Kikuchi, K. Koyama, K. Watanabe, Y. Yamaguchi, R. Kainuma, T. Kanomata, J. Alloys Comp. **580**, 506 (2013)
17. S. Fabbrici, G. Porcari, F. Cugini, M. Solzi, J. Kamarad, Z. Arnold, R. Cabassi, F. Albertini, Entropy **16**, 2204 (2014)
18. K. Das, T.K. Bandyopadhyay, S. Das, J. Mater. Sci. **37**, 3881 (2002)
19. Quantum ESPRESSO package Version 5.02 (2014) at http://www.pwscf.org
20. J.P. Perdew, K. Burke, M. Enzerhof, Phys. Rev. Lett. **77**, 3865 (1996)

21. P. Entel, M.E. Gruner, D. Comtesse, V. Sokolovskiy, V. Buchelnikov, Phys. Status Solidi B **251**, 2135 (2014)
22. V.D. Buchelnikov, V.V. Sokolovskiy, M.A. Zagrebin, M.A. Tufatullina, P. Entel, J. Phys. D: Appl. Phys. **48**, 164005 (2015)